AD-A082 126 VIRGINIA UNIV CHARLOTTESVILLE DEPT OF MATERIALS SCIENCE F/G 11/6
IN-SITU HVEM INVESTIGATION OF PROCESSES LEADING TO FRACTURE IN --ETC(U)
FEB 80 H G WILSDORF N00014-75-C-0855
UNCLASSIFIED UVA/525323/MS80/105 NL

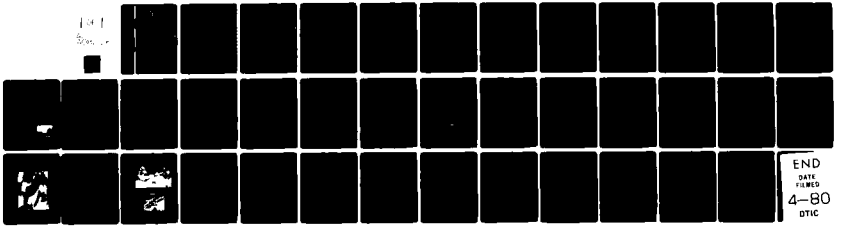

END
DATE FILMED
4-80
DTIC

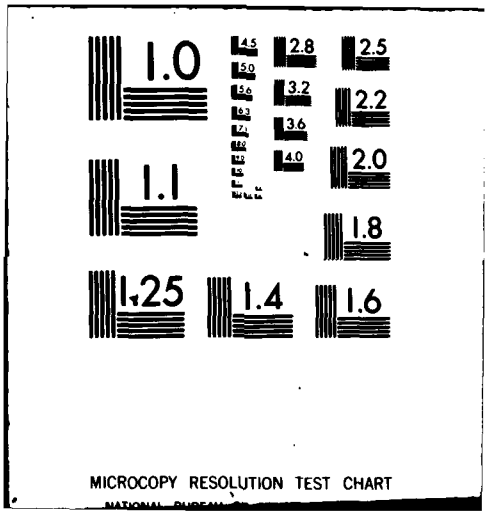
1.0
1.1
1.25
1.4
1.6
1.8
2.0
2.2
2.5
2.8
3.2
3.6
4.0
4.5
5.0
5.6
6.3
7.1
MICROCOPY RESOLUTION TEST CHART

AD A082126

DDC FILE COPY

LEVEL II

RESEARCH LABORATORIES FOR THE ENGINEERING SCIENCES

SCHOOL OF ENGINEERING AND APPLIED SCIENCE

UNIVERSITY OF VIRGINIA

Charlottesville, Virginia 22901

DTIC
MAR 19 1980
S
C

A Technical Report
on Grant No. N00014-75-C-0855

IN-SITU INVESTIGATION OF PROCESSES LEADING TO FRACTURE IN METALS

Submitted to:

Office of Naval Research
800 N. Quincy Street
Arlington, Virginia 22217

Submitted by:

H. G. F. Wilsdorf
Professor

This document has been approved for public release and sale; its distribution is unlimited.

Report No. UVA/525323/MS80/105
February 1980

80 2 20 022

RESEARCH LABORATORIES FOR THE ENGINEERING SCIENCES

Members of the faculty who teach at the undergraduate and graduate levels and a number of professional engineers and scientists whose primary activity is research generate and conduct the investigations that make up the school's research program. The School of Engineering and Applied Science of the University of Virginia believes that research goes hand in hand with teaching. Early in the development of its graduate training program, the School recognized that men and women engaged in research should be as free as possible of the administrative duties involved in sponsored research. In 1959, therefore, the Research Laboratories for the Engineering Sciences (RLES) was established and assigned the administrative responsibility for such research within the School.

The director of RLES—himself a faculty member and researcher—maintains familiarity with the support requirements of the research under way. He is aided by an Academic Advisory Committee made up of a faculty representative from each academic department of the School. This Committee serves to inform RLES of the needs and perspectives of the research program.

In addition to administrative support, RLES is charged with providing certain technical assistance. Because it is not practical for each department to become self-sufficient in all phases of the supporting technology essential to present-day research, RLES makes services available through the following support groups: Machine Shop, Instrumentation, Facilities Services, Publications (including photographic facilities), and Computer Terminal Maintenance.

A Technical Report

IN-SITU HVEM INVESTIGATION OF PROCESSES LEADING TO FRACTURE IN METALS

Submitted to:

Office of Naval Research
800 N. Quincy Street
Arlington, Virginia 22217

Submitted by:

H. G. F. Wilsdorf
Professor

Department of Materials Science
RESEARCH LABORATORIES FOR THE ENGINEERING SCIENCES
SCHOOL OF ENGINEERING AND APPLIED SCIENCE
UNIVERSITY OF VIRGINIA
CHARLOTTESVILLE, VIRGINIA

Report No. UVA/525323/MS80/105
February 1980

Copy No. 8

This document has been approved for public release and sale; its distribution is unlimited.

(9) Technical rept 1 Mar 76 - 31 Mar 80

SECURITY CLASSIFICATION OF THIS PAGE (When Data Entered)

REPORT DOCUMENTATION PAGE	READ INSTRUCTIONS BEFORE COMPLETING FORM
1. REPORT NUMBER	2. GOVT ACCESSION NO. / 3. RECIPIENT'S CATALOG NUMBER
4. TITLE (and Subtitle): (6) In-Situ HVEM Investigation of Processes Leading to Fracture in Metals	5. TYPE OF REPORT & PERIOD COVERED: Technical Report 3/1/76 - 3/31/80
	6. PERFORMING ORG. REPORT NUMBER: (14) UVA/525323/MS80/105
7. AUTHOR(s): (10) H. G. F. Wilsdorf	8. CONTRACT OR GRANT NUMBER(s): (15) N00014-75-C-0855
9. PERFORMING ORGANIZATION NAME AND ADDRESS: University of Virginia, Charlottesville, Virginia 22901	10. PROGRAM ELEMENT, PROJECT, TASK AREA & WORK UNIT NUMBERS: (12) 139
11. CONTROLLING OFFICE NAME AND ADDRESS: Office of Naval Research, 800 N. Quincy Street, Arlington, VA 22217	(11) 12. REPORT DATE: Feb 1980; 13. NUMBER OF PAGES: 23
14. MONITORING AGENCY NAME & ADDRESS (if different from Controlling Office)	15. SECURITY CLASS. (of this report); 15a. DECLASSIFICATION/DOWNGRADING SCHEDULE

16. DISTRIBUTION STATEMENT (of this Report)

This document has been approved for public release and sale; its distribution is unlimited.

17. DISTRIBUTION STATEMENT (of the abstract entered in Block 20, if different from Report)

18. SUPPLEMENTARY NOTES

19. KEY WORDS (Continue on reverse side if necessary and identify by block number)

ALPHA

20. ABSTRACT (Continue on reverse side if necessary and identify by block number)

The unique features of in-situ straining to fracture in high voltage electron microscopes have been outlined. Phenomena pertinent to the ductile fracture of metals have been reviewed as they relate to the study of rupture in the microstructural regime. Experimental observations on pure single crystals of silver, α-iron, and beryllium during fracture have been reported and analyzed. The fracture mechanism can be subdivided into the sequence microvoid initiation, void growth, and void coalescence

DD FORM 1 JAN 73 1473 EDITION OF 1 NOV 65 IS OBSOLETE

SECURITY CLASSIFICATION OF THIS PAGE (When Data Entered)

401762

TOB

It is proposed to distinguish between a primary and a secondary sequence. The latter is applicable to ligament fracture which constitutes the final separation. It was concluded that dislocation cell walls and other boundaries are the initiation sites for microcracks in pure metals and alloys.

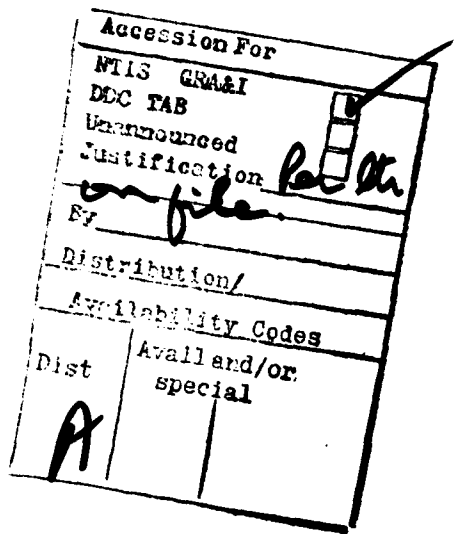

SECTION I

INTRODUCTION

Fracture proceeds by the propagation of cracks and thus is a dynamic process. Although it must have been obvious for a long time that a continuous recording of phenomena occurring at the crack tip should be of great value, little effort has been expanded on dynamic experiments. Most of the data available in the literature is related to fracture energy, specimen geometry and fracture surfaces.

While brittle fracture can be handled satisfactorily from a viewpoint of energy requirements to create new surface, ductile fracture is far more involved. Here, crack initiation is preceded by a substantial amount of plastic deformation which immediately directs our attention to microstructural detail (for a review see Patterson and Wilsdorf). Lattice and crystal defects play important roles during deformation and one realizes that the proven power of continuum mechanics to understand brittle failure is diminished when it comes to the exploration of the mechanism of ductile fracture. The development of a quantitative theory of workhardening for metals is one of the prerequisites for clarifying the processes leading to rupture in metals. The other development that was needed to advance the field is related to modern electron microscopy. The first in-situ deformation of metals was carried out in 1957 in a 100 kV electron microscope by Wilsdorf (1958); some aluminum specimens also were fractured at that time but little information of value to the fracture process could be obtained on account of limiting experimental conditions. The development of high voltage electron

microscopy (HVEM) finally provided an experimental tool to study dynamic processes of fracture in the microstructural regime. The behavior of dislocations and plastic deformation in metals using HVEM in-situ techniques were studied extensively by Imura at Nagoya University and by Fujita at Osaka University, while the research group at the University of Virginia concentrated on ductile fracture. This paper will relate observations of the latter group to the mechanism of ductile fracture in pure metals and alloys.

SECTION II

EXPERIMENTAL TECHNIQUES

High voltage electron microscopy offers a number of advantages for in-situ straining to fracture in comparison to conventional electron microscopy. Since high energy electrons have a reduced energy exchange with solids, specimen thickness can be substantially increased. Depending on the atomic number of the solid, specimens between 1 μm and 5 μm thick are electron transparent and in most cases allow observations with good resolution. It should be remembered that fracture in ductile metals and alloys begins in the most severely deformed part of the specimens, and one is not concerned with the observation of single dislocations, but rather with plastic deformation in regions having a dislocation density in excess of 10^{10} dislocations/cm^2. Also, one is aiming to view the action in the specimen with diffraction contrast while mass thickness contrast is the limiting contrast mechanism. Consequently, the obtainable resolution depends not only on specimen thickness but to a considerable extent on diffraction conditions.

A second effect of the lower interactions of high energy electrons with matter is reduced contamination of the specimen. It is known that surface films can affect the deformation characteristics of metals and alloys (see for example Rosi, Ruddle and Wilsdorf, Wilsdorf and Ruddle). In-situ straining to fracture primarily involves observations of crack propagation, i.e. the production of new surface. It is conceivable that a heavy contamination could influence the very process under investigation. A high vacuum in the specimen chamber is mandatory in order to ensure that the advantage of HVEM is not diminished. And finally, a

third point can be made which also is a direct consequence of the low loss of energy of HVEM electrons, namely a negligible increase of the specimen's temperature.

However, one important precaution has to be observed. High energy electrons can produce point defects in metals, and it is recommended to ascertain that the displacement threshold for the metal or alloy under investigation is not to be exceeded. While radiation damage normally is of little consequence for post-fracture examination of foils, radiation damage imposed during in-situ straining could affect deformation processes, depending on the length of the experiment which often continues for hours.

Most high voltage electron microscopes have more space in the specimen chamber than conventional instruments which facilitates the operation on tensile stages. The Virginia HVEM has an 8 mm gap between pole pieces and can accommodate any in-situ stage desirable. The microscope was built for side entry stages and the tensile stage consists of a fixed and a movable grip operated through a hydraulic system by means of a rod. Tensile specimens 12 mm x 3 mm can be used and details of the straining stage and examples of specimen preparation have been published earlier by Bauer, Lyles and Wilsdorf.

The recording of a propagating crack and phenomena in front of the crack tip are done by video tape. The TV-camera has incorporated an Orthicon tube which provides for a substantial intensity amplification of the image. The speed is 30 frames per second. The image is taken by the camera directly from the fluorescent screen and with the help of electronic controls a better intensity distribution for the high contrast

images can often be achieved. The recording system for the HVEM at the University of Virginia is shown schematically in Figure 1.

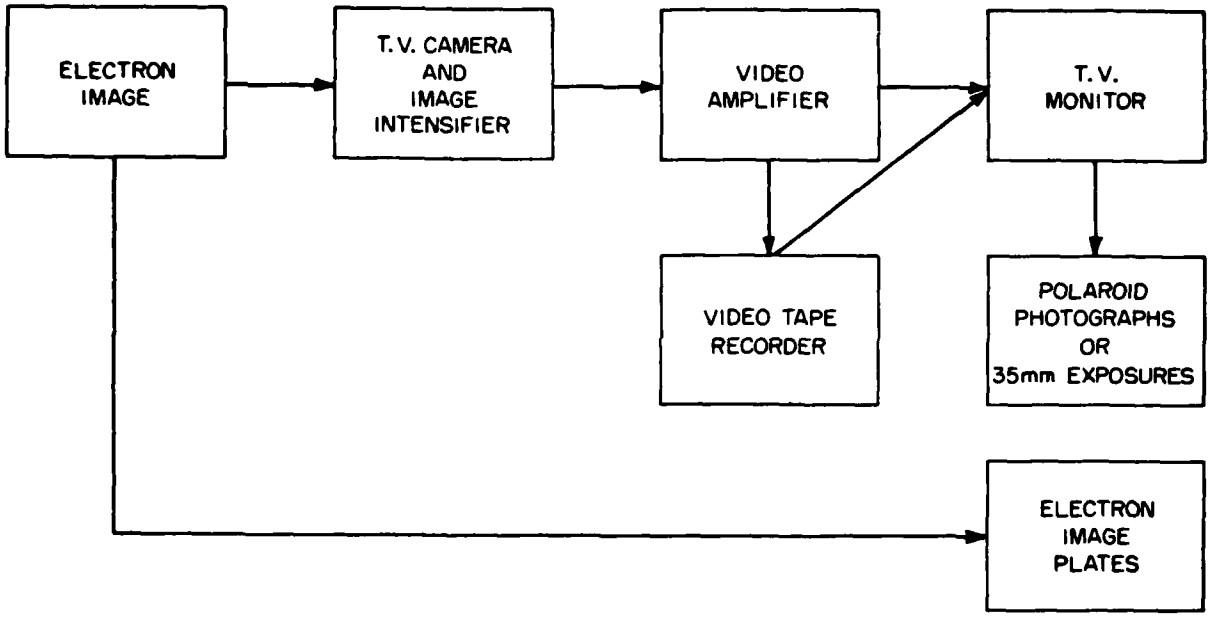

Figure 1. Photographic and video tape recording system for HVEM at the University of Virginia.

SECTION III

GENERAL CONCEPTS

A cylindrical specimen extensively deformed in tension will eventually experience a plastic instability and neck down until fracture is complete. The result is either a "cup and cone" fracture or the necking will continue until the rupture will occur along a chisel edge or at a chisel point. Figures 2a and b demonstrate the two cases at a microscopic scale.

The fracture surface of a "cup and cone" fracture consists firstly of a part which is perpendicular to the stress axis and secondly of shear lips near the surface. The first part is due to the formation of voids which grow until coalescence has been attained. This "fibrous" part is the cross-section of the specimen volume which deformed under triaxial stresses. With the formation of the neck, the uniaxial stress state has to change in order to preserve the conditions of plasticity between the reduced cross-section in the neck and the rest of the specimen. Radial and tangential stresses start from zero values at the surface and increase to maximum values at the center where they become indistinguishable. At the surface one only has axial stresses which, however, must also increase towards the center in order to maintain the plasticity conditions. Near the surface a biaxial stress state exists which produces the shear lips. It should be noted that necking starts when the maximum load has been reached and that the necking strain ε_N is equal to the work hardening exponent n taken from the well known equation for the stress-strain curve $\sigma = k\varepsilon^n$.

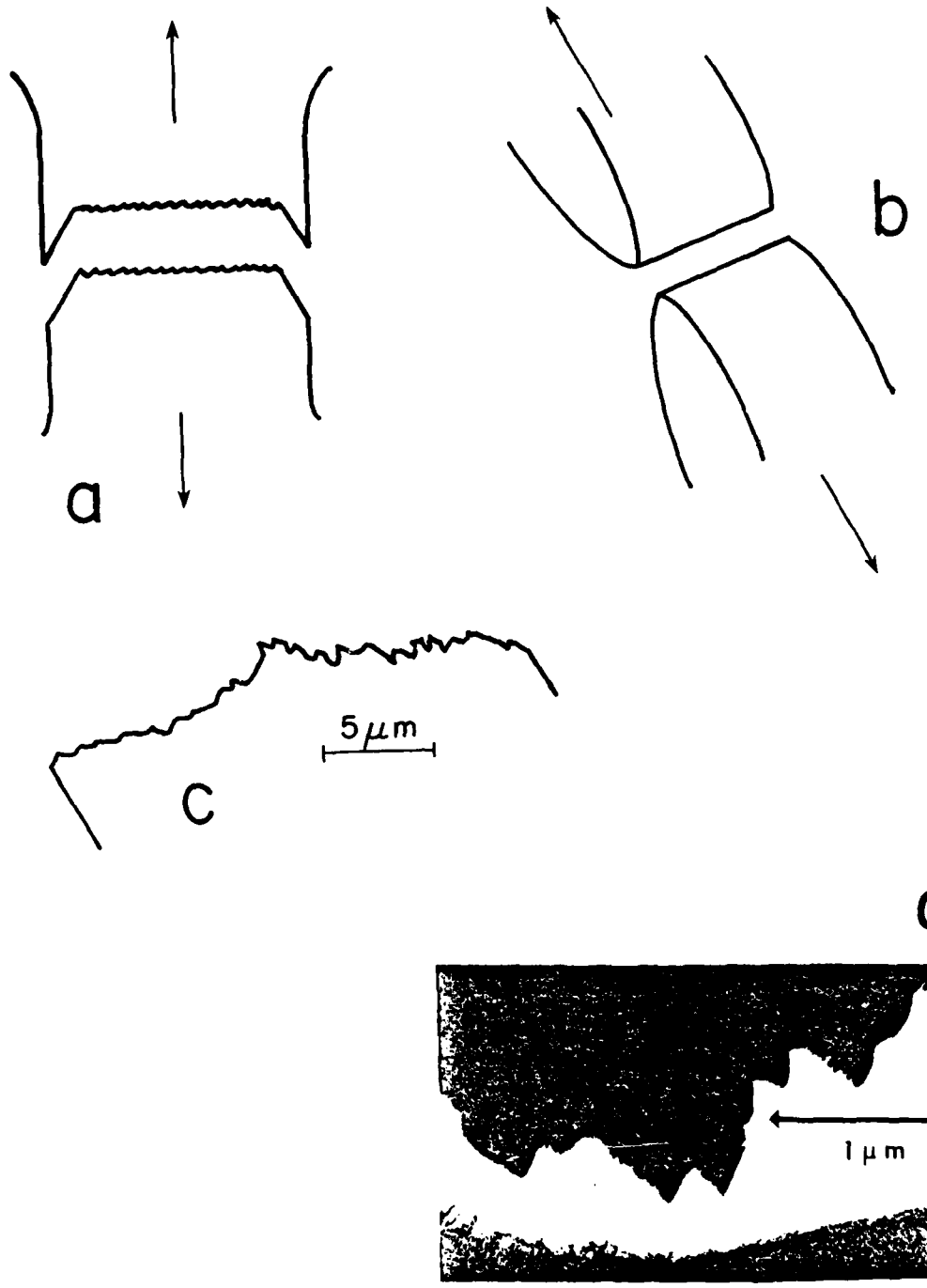

Figure 2. Macroscopic appearance of (a) cup and cone fracture; (b) rupture. Microscopic appearance of chisel edge after rupture (c) in SEM; (d) in TEM, dark field.

Rupture along a chisel edge is thought to be due to shear in the absence of void formation. While the chisel edge in ruptured specimens appears to be straight when viewed in a metallograph, closer examination by scanning electron microscopy (SEM) reveals a ragged edge (Figure 2c). A further increase in magnification by transmission electron microscopy (TEM) shows an even finer zig-zag structure which is partly electron transparent (Figure 2d).

The reason for expecting a straight chisel edge produced by simple shear processes is not unrelated to the traditional view that void initiation in the cup and cone fracture is due to the presence of second phase particles. Then pure shear had to be responsible for the formation of a chisel edge by rupture which indeed was a logical conclusion when considering "pure" metals.

The study of ductile fracture in the microstructural regime was started in earnest only a few decades ago and mostly was carried out on alloys or on metals of commercial purity. An overwhelming number of results showed that the initiation of voids occurred at second phase particles. These results stand undisputed but one has to ask the question: do all voids nucleate at particles or impurity aggregates in alloys and how do voids form in high purity metals and alloys? As a first step, our work concerns the fracture mechanism in pure metals and alloys.

For an understanding of ductile fracture the deformation history of a specimen is of great importance. Since the research to be reported in this paper has been carried out on single crystals, it is appropriate to outline some of the features of work hardening theory of single

crystals which have a direct bearing on the fracture mechanism. With increasing plastic deformation the dislocation density ρ increases as shown by the following equation:

$$\gamma = \rho b \bar{l}$$

with γ the shear strain, b the Burgers vector and $\bar{l}$ the average distance of dislocation travel. The flow stress τ is related to ρ as

$$\tau = \alpha \sqrt{\rho}\ G\ b,$$

α being a constant and G the modulus of rigidity. After the initial deformation through stage I (easy glide) the shear stress-strain curve is almost linear (stage II) until it assumes a parabolic shape (stage III). Fracture terminates stage III.

Clearly, the dislocation patterns developing during stages I and II and in particular in the parabolic stage are of major interest to us since void initiation is taking place almost immediately after work hardening has caused to increase the shear stress to a maximum as mentioned above. As shown by numerous TEM investigations, dislocations arrange themselves into dislocation cell walls from the beginning of stage II through stage III (for references see the review by Thompson). Thus, a three-dimensional dislocation cell arrangement is found throughout the deformed crystal. Kuhlmann-Wilsdorf (1977) has developed a theory of work hardening and recently summarized the salient points of dislocation behavior which leads to the development of dislocation cells. It could be shown that dislocation cell walls are configurations which have the lowest free energy in a work hardened crystal and therefore must occur, provided dislocations can move on a sufficient number of slip systems and can multiply in accordance with the applied stress. The

three-dimensional cell wall configuration consists for the case of single glide deformation of twist and tilt boundaries with the former being parallel and the latter being perpendicular to the slip plane. The stresses exerted by the cell walls are short range and do not extend beyond the cell interiors which they form, but they alternate in sign between neighboring cells. By introducing the principle of similitude into work hardening theory Kuhlmann-Wilsdorf (1968) concluded that new cells are continuously nucleated with increasing stress by the subdivision of the largest cell: experimental evidence exists to show that the cell size decreases inversely with the flow stress as

$$\tau - \tau_o = \alpha\ kGbd^{-1},$$

τ_o being the frictional stress on dislocations, d the cell diameter, and k a constant depending on the material. According to a theory by Holt, the cell size is inversely proportional to $\sqrt{\rho}$ which has been verified experimentally by Ambrosi et. al.

The above discussion relates to bulk crystals and it appears appropriate to inquire whether specimens with the reduced size used in HVEM in-situ straining behave in accordance with theory. The first known experiments on metals strained in an electron microscope were carried out as early as 1957 at 100 kV (Wilsdorf, 1958). The presence of dislocation sub-boundaries and their behavior under tensile stresses were the most obvious phenomena in aluminum foils approximately 0.1 μm thick. Evidence for the multiplication sites of dislocations in thin foils was published shortly afterwards (Wilsdorf, 1959); it was shown that dislocation sources in cells walls, twin boundaries and grain boundaries were providing the dislocations which sustained the plastic flow in the

foils. More recently, other direct observations on cell walls in thin foils produced under stress in the HVEM were made by Fujita and Yamada, Imura, Saka and Yukawa, and by Pollock; Tabata, Yamanaka and Fujita confirmed the above relationship between stress and cell size. Also, these authors compared dislocation cell structures in thin foils of aluminum and bulk specimens with satisfactory results. It can be concluded that the cell structures as predicted by theory and found in bulk specimens will also be produced in specimens employed for in-situ fracture in the HVEM.

SECTION IV

EXPERIMENTAL RESULTS

General Comments

An understanding of the mechanisms leading to rupture is greatly aided by subdividing the possible processes into the sequence void initiation - void growth - void coalescence. After the neck is formed voids initiate in this most heavily work hardened area of the specimen and develop into a void sheet. At this point the specimen is held together by ligaments which are continuously elongated with the simultaneous growth of the voids. The coalescence of voids actually will be completed by straining thin ligaments to fracture. Again, the sequence void initiation - growth - coalescence may serve as a guideline although it may be more appropriate to talk about hole initiation depending on how severely the thickness of the ligaments has been reduced. The sequences will be referred to as primary or secondary depending on whether thick specimens or ligaments are under consideration. As will be shown in this chapter, both types of specimen have been investigated demonstrating the validity of applying the concept of a primary or secondary sequence.

Beryllium

Beryllium was chosen for in-situ experiments on account of its low atomic number and its hexagonal structure. Crystals with a thickness of up to 3 μm are electron transparent and therefore lend themselves for fracture research. The specimens were obtained from a zone refined high purity single crystal through acid saw cutting and electropolishing.

All results discussed here have been obtained from tensile specimens oriented for prism slip. The crosshead speed of the tensile apparatus was adjusted in the range 10^{-6} - 10^{-4} cm/sec, depending on the purpose of the experiment.

Pollock in his dissertation investigated the dislocation cell structure which indeed developed according to theoretical concepts. The average cell size peaked at 1.5 μm in the vicinity of the crack tip although cells with more than 3 μm and some smaller than 0.5 μm were discernable. The widths of cell walls are difficult to estimate since their inclination against the surface of the foil have not been determined as yet. Thus the smaller values which rarely exceeded 0.1 μm are more significant. Rotations between individual cells were found to vary between 5^{o} and 21^{o}.

The most significant observations of Pollock's fracture studies relate to the initiation of the first microcracks. They were found to occur along cell walls as illustrated in a drawing, Figure 3, which was taken from micrographs published earlier by Gardner, Pollock and Wilsdorf. Figure 3a shows the cell structure and Figure 3b includes the opening of a microcrack after the strain increment; it should be noted that the cell structure has undergone changes, although major features of the cell structure have remained unchanged. Normally, more than one microcrack initiates in a shear zone. Growth of microcracks occurs by slip until fracture is complete.

α-Iron

The iron crystals subjected to fracture were obtained by an ion reduction technique described by Gardner (1978). It was possible to

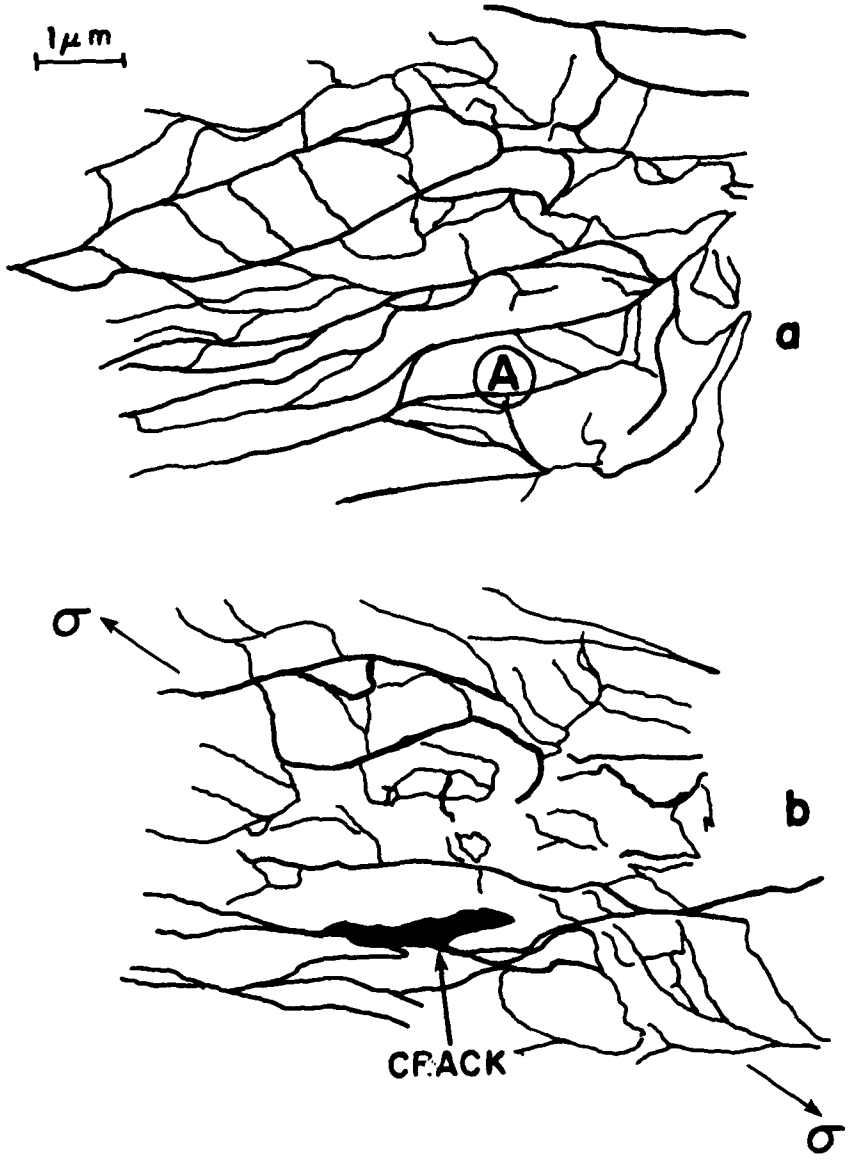

Figure 3. Schematic representation of microcrack initiation at dislocation cell walls A in Beryllium (according to micrographs by Pollock).

produce single crystals with shapes suitable for in-situ straining with thicknesses between 0.1 μm and 100 μm. Crystals with orientations parallel to <111>, <100>, <011>, and <211> necked down after prolonged elongation to a chisel edge. Gardner (1977) determined the glide processes involved and was able to predict the orientation of the chisel edge for different crystal axes.

The macroscopic shape of the chisel edge at a fractured crystal looks like Figure 2b and a number of micrographs have been published earlier by Pollock et. al., and Gardner and Wilsdorf. The microscopic appearance of the chisel edge is extremely irregular as shown in Figures 2c and d. Iron is known to develop dislocation cells during plastic deformation although there are differences between FCC and BCC cell structures which have been discussed by Thompson. It was found in our experiments that the dislocation density along the submicroscopical chisel edge was extremely high and dislocation cells were not clearly resolvable. However, diffraction contrast in high resolution images showed separate volume elements in the order of a few hundred angstroms. Selected area diffraction with a 150 nm diameter beam showed point diffraction patterns consisting of three or four patterns with different zone axes; also micro-twinning was found by Gardner (1977). Reducing the beam diameter to 40 nm, diffraction patterns along the edge of the fractured ligaments again showed substantial rotations of volume elements against each other and occasionally micro-twinning. In many instances the intensity of the primary beam is not higher than that of the strongest diffracted beams which indicated the presence of an extremely high defect density. Misorientations of up to 35^{o} have

been measured. Often the chisel edge appears in TEM with a zigzag shape and one can discern through thickness fringe contrast that the individual parts sticking out from a generally definable crack flank are thinner towards the edges but not below a value of about a few hundred angstroms.

Silver

Single crystals of silver were grown as thin ribbons by ion reduction. They often reached a length of 5×10^{-1} cm, a width of 1×10^{-1} cm, and varied in thickness between 0.2 μm and 7 μm. The long direction of the ribbons was parallel to <110> and the large surface was the {111} plane. Details of growth and purity of the crystals and specimen preparation have been described by Lyles. All crystals showed transverse necking with subsequent severe deformation in the neck; as expected from glide geometry the crystal axis rotated by a maximum of 30° and assumed a <211> direction. A complete analysis of glide processes to explain the plastic behavior of the crystals preceding fracture was successful and proved to be essential for an understanding of the sequence leading to rupture.

Cracks started normally at the edge of the ribbon in the necked area and proceeded under 60° against the $[\bar{2}11]$ tensile axis parallel to $[11\bar{2}]$. Microcracks were seen to open up in front of the propagating crack tip which grew in time into larger holes with the exact geometrical shape of parallelograms. The microcracks started as narrow slits about 0.2 μm long parallel to <110>. Their enlargement occurred both in length and width assuming first a trapezoidal shape until a parallelogram

was completed, the sides of which were lying parallel to projections of the two glide systems with the highest Schmid factors as discussed by Lyles and Wilsdorf. The initiation of holes ahead of the crack tip was videotaped and some interesting observations and measurements resulted: Microcracks invariably started as slits parallel to <110> in fairly regular intervals of about 0.5 μm. The initiation site normally was recognizable by an elongated narrow dark band due to diffraction contrast. With a crosshead speed of 10^{-5} *cm/sec the microcrack* appeared in less than 0.5 seconds after first seeing the contrast line. Coalescence of the holes took place after the holes had grown into parallelograms with narrow ligaments separating them. The final coalescence could be followed at resolutions which permitted to see the motion of small groups of dislocations.

SECTION V

DISCUSSION AND CONCLUSIONS

The experiments summarized in the preceding chapter illustrate that in-situ straining to fracture in a HVEM can provide unique information regarding the fracture mechanism operating in pure ductile metals. Understanding both the primary and secondary sequence of void initiation - void growth - void coalescence has been facilitated greatly. While there are obvious similarities between the primary and secondary sequence, major differences also exist. The processes in the primary sequence occur in a triaxial stress field as far as void initiation and growth are concerned. By the time the void sheet has developed and the crystal is being held together by a multitude of thin ligaments, the deformation of these ligaments must continue under plane stress conditions. Thus the secondary sequence operates under a different system of stresses due to the reduced thickness of the ligaments.

How does this difference in thickness affect the behavior of dislocations and point defects? The primary sequence operates in bulk, i.e. external distances are millions of atomic diameters away from the center. For the secondary sequence these distances number only a few hundred atomic diameters. Since dislocation densities observed in ductile fracture are extremely high, image forces will not play a role in either sequence. However, based on considerations by Wilsdorf and Kuhlmann-Wilsdorf the production of point defects by glide cannot be neglected nor the difference between dislocation - defect interactions.

It is generally agreed that point defects are being generated during plastic flow in crystals and a number of mechanisms have been proposed by Seitz, Read, Kuhlmann-Wilsdorf (1960), and Kuhlmann-Wilsdorf and Wilsdorf. Although point defects generated in one or another fashion will interact with dislocations or nearby sinks, it has been calculated that vacancies will predominate over interstitials. Besides the effects of vacancy interactions with dislocations as worked out by Kuhlmann-Wilsdorf and Wilsdorf, it can be expected that vacancies remain in the crystal at a notable supersaturation. Since the dislocation distribution changes its scale as $(\tau-\tau_0)^{-1}$, with τ and τ_0 being the applied and frictional shear stress respectively, one might expect that the void distribution follows this law correspondingly, if indeed the indicated relationship between dislocations, vacancies and voids should exist. A careful study of SEM fractographs has been made by Bauer and Wilsdorf who counted the inter void spacings for 304 stainless steel foils fractured at increasing stresses. The measurements agreed with the above law, and it was concluded that voids arising from dislocation produced vacancies could be responsible for microcrack initiation in bulk crystals.

In-situ fracture experiments in the HVEM cover a broad range of specimen thicknesses from about 5 μm down to 10 or 20 nm. From the viewpoint of fracture research in the microstructural regime a crystal a few micrometers thick could indeed follow the primary sequence. If one takes as a criterion the appearance of dimples in SEM fractographs, stainless steel foils 3.76 μm thick (Bauer) and silver crystals 2 μm thick

(Lyles) would still be considered as "thick" specimens for mechanism of void initiation and growth.

It is clear, however, that the final separation in ductile fracture occurs by the rupture of ligaments which can have a range of thicknesses. SEM fractographs show in general rather shallow dimples which are supposed to represent one half of a void. The question of the whereabouts of the ligaments seems not to have been raised. In a rare fractograph, Figure 4, Hedke has been able to show extensive ligaments in beryllium. Their length is seen to be 10 μm to 20 μm while their thickness is judged mostly well below 0.1 μm. One ligament is so thin that it is not interfering with the scattering processes of the primary 25 kV electrons (see arrow). If this micrograph is somewhat representative for fracture surfaces, one must conclude that normally the final ligaments are too thin and unstable to keep their shape, and therefore fold over and become lost for detection by SEM due to limitation of resolution.

In comparison to other microscopic techniques in-situ HVEM allows one to discern in great detail the processes which are involved in the final failure under actual dynamic conditions. The fact that ligaments are electron transparent provides a unique opportunity to study the decisive role played by crystal defects in the final separation. As a matter of fact, filming crack propagation in silver ribbons allowed to observe the complete secondary sequence. Microcracks open in front of the crack tip, the growth of microcracks can be recorded in time and the coalescence between them can be seen in great detail. The latter process was analyzed by Lyles and Wilsdorf. Calculations showed that

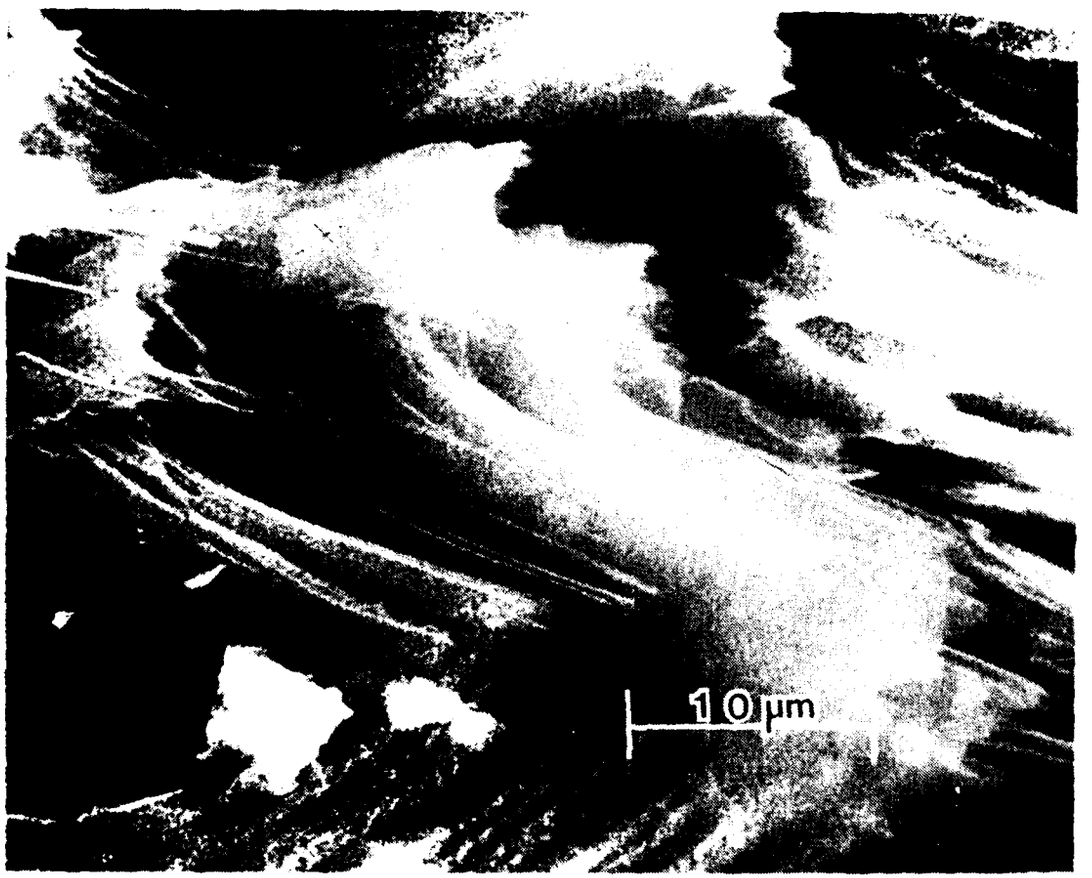

Figure 4. Ligaments produced by ductile fracture of Beryllium crystal deformed in tension along $[11\bar{2}0]$, as seen by SEM. Courtesy of D. L. Hedke.

ligaments between holes are being reduced in width and thickness until the ligament becomes too thin to permit the operation of dislocation sources at the local stress level. This means however, that these ligaments can sustain high stresses. Coalescence occurs eventually when dislocations generated in the thicker crack flank move through the very thin final remains of ligaments, i.e. separation is by shear.

This result is in agreement with theory since shear energy is considerably less than decohesion energy. On the other hand it appears that microcrack initiation takes place in tension and not by shear. In silver, microcracks open up suddenly as narrow slits about 0.2 μm long in the most work hardened area ahead of the crack tips; in α-iron the work hardened area near the final separation consists of small volume elements with misorientations between 20 and 30^{o}; in beryllium direct HVEM observations show that microcracks form along dislocation cell walls. While there can hardly be any doubt that microcrack formation in beryllium takes place in tension, the work on α-iron needs some elaboration. Figure 5 gives an impression of the structure at the crack flank as seen by TEM. Volume elements in the order of a few hundred angstroms with widely different orientations are discernable by diffraction contrast and it is concluded that the boundaries between the most misoriented volume elements are the sites of microcrack initiation. This conclusion is a logical one since the decohesion energy $W_{dec} \cong 2\gamma_s - \gamma_b$, with γ_s the surface free energy and γ_b the energy of a boundary. The observations on silver are in agreement with this concept. There are no reliable measurements of the energy of dislocation cell walls as yet in the literature, but it should be noted that the misorientations of sub-

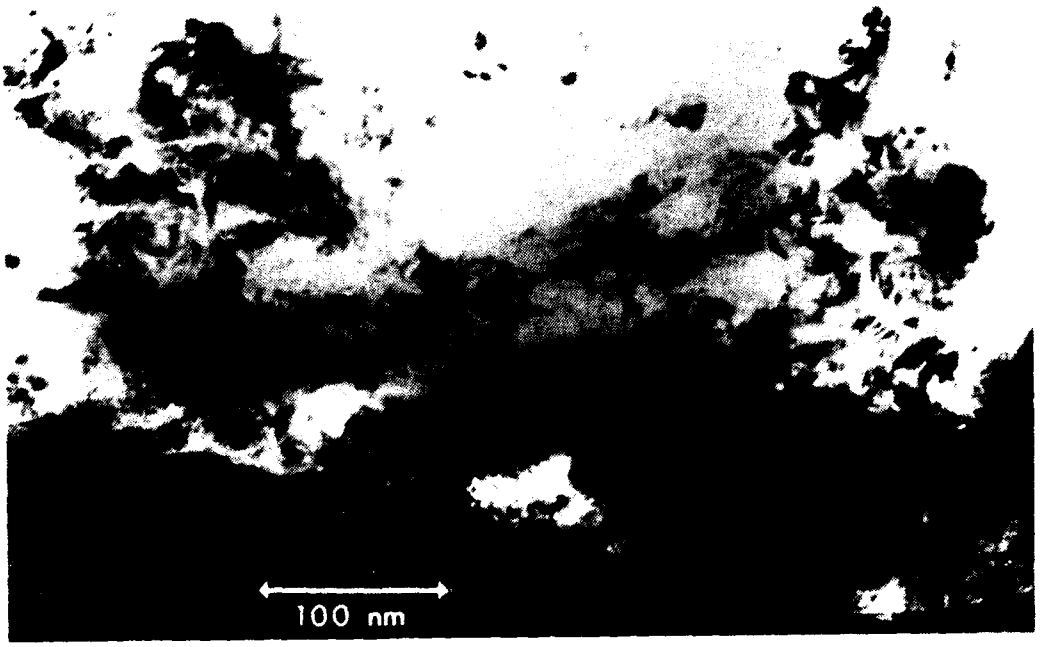

Figure 5. Heavily work hardened region near crack flank in α-iron crystal. TEM permits to discern small volume elements rotated against each other through diffraction contrast.

Figure 6. Initiation of microcrack at twin boundary in work hardened area of 304 stainless steel foil, as seen by TEM. Courtesy of R. W. Bauer.

grains etc. near the crack flank are substantial and therefore could approach the energy of grain boundaries. Thus, the amount of W_{dec} can be expected to have declined effectively by γ_b.

In polycrystalline metals and alloys of high purity, complications to the above mechanism will arise. However, Figure 6 shows that in polycrystalline austenitic stainless steel, crack initiation also started at a boundary, in this case a twin boundary. Dislocation cell wall formation in alloys is more difficult, since a lower stacking fault energy reduces cross-slip and ability of dislocations to move freely on different slip planes.

This review has attempted to show that in-situ HVEM has a place in the microstructural regime of fracture research. Video tape recordings of crack propagation speeds, phenomena related to plastic deformation in front of the crack tip, and complementary investigations by SEM and microdiffraction will continue to be instrumental in the search for a better understanding of ductile fracture.

REFERENCES

Ambrosi, P., Gottler, E., Schwink, C. H.: Scripta Met. 8, 1093 (1974).

Bauer, R. W.: Ductile Fracture in 304 Stainless Steel Rolled Foils. Dissertation. University of Virginia, 1975.

Bauer, R. W., Lyles, R. L., Wilsdorf, H. G. F.: ZS Metallkd. 63, 525 (1972).

Bauer, R. W., Wilsdorf, H. G. F.: Scripta Met. 7, 1213 (1973).

Fujita, H.: J. Phys. Soc. Japan 26, 331 (1969).

Fujita, H., Yamada, H.: Trans. Japan Inst. Metals 9 (Suppl.), 943 (1968).

Gardner, R. N.: Ductile Fracture Initiation in Pure α-Iron. Dissertation. University of Virginia, 1977.

Gardner, R. N.: J. Cryst. Growth 43, 425 (1978).

Gardner, R. N., Pollock, T. C., Wilsdorf, H. G. F.: Matls. Sci. Eng. 29, 169 (1977).

Gardner, R. N., Wilsdorf, H. G. F.: Proc. 4th Int. Conf. Fracture, Ed. Taplin, U. Waterloo Press, Waterloo, Vol. 2, 349 (1977).

Hedke, D. E.: Dislocation Cell Characterization in Beryllium Fracture. M.S. Thesis. University of Virginia, 1979.

Holt, D. L.: J. Appl. Phys. 41, 3197 (1970).

Imura, T.: Structure and Properties of Materials, Ed. Thomas, U. Calif. Press, Berkeley, 1972, pp. 104.

Imura, T., Saka, H., Yukawa, N.: Japan J. Appl. Phys. 8, 405 (1969).

Kuhlmann-Wilsdorf, D.: Phys. Rev. 120, 773 (1960).

Kuhlmann-Wilsdorf, D.: Workhardening, Eds. Hirth and Weertman, Gordon and Breach, New York, 1968, pp. 97.

Kuhlmann-Wilsdorf, D.: Workhardening in Tension and Fatigue, Ed. Thompson, AIME, New York, 1977, pp. 1.

Kuhlmann-Wilsdorf, D., Wilsdorf, H. G. F.: Electron Microscopy and the Strength of Crystals. Ed. Thomas and Washburn, John Wiley, New York, 1963, pp. 575.

Lyles, R. L., Jr.: The Submicroscopic Fracture Mechanism of Silver Crystals. M.S. Thesis, University of Virginia, 1971.

Lyles, R. L., Jr., Wilsdorf, H. G. F.: Acta Met. 23, 269 (1975).

Patterson, R. L., Wilsdorf, H. G. F.: Fracture, Ed. Liebowitz, Acad. Press, New York, 1968, Vol. I, pp. 183.

Pollock, T. C.: The Fracture of Beryllium Single Crystals. Dissertation. University of Virginia, 1977.

Read, W. T.: Dislocations in Crystals, McGraw-Hill, New York, 1953, pp. 85.

Rosi, F. D.: Acta Met. 5, 348 (1957).

Ruddle, G. E.: The Influence of Thin Epitaxial Surface Films on the *Plastic Properties of Copper. Dissertation. University of Virginia,* 1969.

Seitz, F.: Advances in Physics 1, 43 (1952).

Tabata, T., Yamanaka, S., Fujita, H.: Acta Met. 26, 405 (1978).

Thompson, A. W.: Met. Trans. 8A, 833 (1977).

Wilsdorf, H. G. F.: ASTM Spec. Tech. Publ. 245, 43 (1958).

Wilsdorf, H. G. F.: Structure and Properties of Thin Films, Eds. Neugebauer, Newkirk, Yermilyea, John Wiley Sons, New York, 1959,pp. 151.

Wilsdorf, H. G. F., Kuhlmann-Wilsdorf, D.: Phys. Rev. Letters 3, 170 (1959).

Wilsdorf, H. G. F., Ruddle, G. E.: Surface Effects in Crystal Plasticity. Eds. Latanision and Fourie, Noordhoff, Leyden, 1977, pp. 565.

DISTRIBUTION LIST

Copy No.	
1 - 3	Office of Naval Research 800 N. Quincy Street Arlington, Virginia 22217
4 - 61	See Basic Distribution List
62 - 88	See Supplementary Distribution List
89 - 90	H. G. F. Wilsdorf
91	K. R. Lawless
92	I. A. Fischer Office of Sponsored Programs
93 - 94	E. H. Pancake Clark Hall
95	RLES Files

0555:jt

BASIC DISTRIBUTION LIST

Technical and Summary Reports

Organization	No. of Copies
Defense Documentation Center Cameron Station Alexandria, Virginia 22314	(12)
Office of Naval Research Department of the Navy	
Attn: Code 471	(1)
Code 102	(1)
Code 470	(1)
Commanding Officer Office of Naval Research Branch Office 495 Summer Street Boston, Massachusetts 02210	(1)
Commanding Officer Office of Naval Research Branch Office 536 South Clark Street Chicago, Illinois 60605	(1)
Office of Naval Research San Francisco Area Office 760 Market Street, Room 447 San Francisco, California 94102 Attn: Dr. P. A. Miller	(1)
Naval Research Laboratory Washington, D.C. 20390	
Attn: Code 6000	(1)
Code 6100	(1)
Code 6300	(1)
Code 6400	(1)
Code 2627	(1)
Naval Air Development Center Code 302 Warminster, Pennsylvania 18974 Attn: Mr. F. S. Williams	(1)
Naval Air Propulsion Test Center Trenton, New Jersey 08628 Attn: Library	(1)
Naval Construction Batallion Civil Engineering Laboratory Port Hueneme, California 93043 Attn: Materials Division	(1)
Naval Electronics Laboratory Center San Diego, California 92152 Attn: Electron Materials Sciences Division	(1)
Naval Missile Center Materials Consultant Code 3312-1 Point Mugu, California 93041	(1)
Commanding Officer Naval Surface Weapons Center White Oak Laboratory Silver Spring, Maryland 20910 Attn: Library	(1)
David W. Taylor Naval Ship R&D Center Materials Department Annapolis, Maryland 21402	(1)
Naval Undersea Center San Diego, California 92132 Attn: Library	(1)
Naval Underwater System Center Newport, Rhode Island 02840 Attn: Library	(1)
Naval Weapons Center China Lake, California 93555 Attn: Library	(1)
Naval Postgraduate School Monterey, California 93940 Attn: Mechanical Engineering Dept.	(1)
Naval Air Systems Command Washington, D.C. 20360	
Attn: Code 52031	(1)
Code 52032	(1)
Code 320	(1)

BASIC DISTRIBUTION LIST (Cont'd)

Organization	No. of Copies
Naval Sea System Command Washington, D.C. 20362 Attn: Code 035	(1)
Naval Facilities Engineering Command Alexandria, Virginia 22331 Attn: Code 03	(1)
Scientific Advisor Commandant of the Marine Corps Washington, D.C. 20380 Attn: Code AX	(1)
Naval Ship Engineering Center Department of the Navy CTR BG #2 3700 East-West Highway Prince Georges Plaza Hyattsville, Maryland 20782 Attn: Engineering Materials and Services Office, Code 6101	(1)
Army Research Office Box CM, Duke Station Durham, North Carolina 27706 Attn: Metallurgy & Ceramics Div.	(1)
Army Materials and Mechanics Research Center Watertown, Massachusetts 02172 Attn: Res. Programs Office (AMXMR-P)	(1)
Air Force Office of Scientific Research Bldg. 410 Bolling Air Force Base Washington, D.C. 20332 Attn: Chemical Science Directorate Electronics and Solid State Sciences Directorate	(1) (1)
Air Force Materials Lab (LA) Wright-Patterson AFB Dayton, Ohio 45433	(1)
NASA Headquarters Washington, D.C. 20546 Attn: Code RRM	(1)
NASA Lewis Research Center 21000 Brookpark Road Cleveland, Ohio 44135 Attn: Library	(1)
National Bureau of Standards Washington, D.C. 20234 Attn: Metallurgy Division Inorganic Materials Division	(1) (1)
Defense Metals and Ceramics Information Center Battelle Memorial Institute 505 King Avenue Columbus, Ohio 43201	(1)
Director Ordnance Research Laboratory P.O. Box 30 State College, Pennsylvania 16801	(1)
Director Applied Physics Laboratory University of Washington 1013 Northeast Fortieth Street Seattle, Washington 98105	(1)
Metals and Ceramics Division Oak Ridge National Laboratory P.O. Box X Oak Ridge, Tennessee 37380	(1)
Los Alamos Scientific Laboratory P.O. Box 1663 Los Alamos, New Mexico 87544 Attn: Report Librarian	(1)
Argonne National Laboratory Metallurgy Division P.O. Box 229 Lemont, Illinois 60439	(1)

BASIC DISTRIBUTION LIST (Cont'd)

Organization	No. of Copies	Organization	No. of Copies
Brookhaven National Laboratory Technical Information Division Upton, Long Island New York 11973 Attn: Research Library	(1)		
Library Building 50 Room 134 Lawrence Radiation Laboratory Berkeley, California	(1)		

SUPPLEMENTARY DISTRIBUTION LIST

Technical and Summary Reports

Dr. T. R. Beck
Electrochemical Technology Corporation
10035 31st Avenue, NE
Seattle, WA 98125

Professor I. M. Bernstein
Carnegie-Mellon University
Schenley Park
Pittsburgh, PA 15213

Professor H. K. Birnbaum
University of Illinois
Department of Metallurgy
Urbana, IL 61801

Dr. Otto Buck
Rockwell International
1049 Camino Dos Rios
P.O. Box 1085
Thousand Oaks, CA 91360

Dr. David L. Davidson
Southwest Research Institute
8500 Culebra Road
P.O. Drawer 28510
San Antonio, TX 78284

Dr. D. J. Duquette
Department of Metallurgical Engineering
Rensselaer Polytechnic Institute
Troy, NY 12181

Professor R. T. Foley
The American University
Department of Chemistry
Washington, DC 20016

Mr. G. A. Gehring
Ocean City Research Corporation
Tennessee Avenue & Beach Thorofare
Ocean City, NJ 08226

Dr. J. A. S. Green
Martin Marietta Corporation
1450 South Rolling Road
Baltimore, MD 21227

Professor R. H. Heidersbach
University of Rhode Island
Department of Ocean Engineering
Kingston, RI 02881

Professor H. Herman
State University of New York
Material Sciences Division
Stony Brook, NY 11794

Professor J. P. Hirth
Ohio State University
Metallurgical Engineering
Columbus, OH 43210

Dr. D. W. Hoeppner
University of Missouri
College of Engineering
Columbia, MO 65201

Dr. E. W. Johnson
Westinghouse Electric Corporation
Research and Development Center
1310 Beulah Road
Pittsburgh, PA 15235

Dr. F. Mansfeld
Rockwell International Science Center
1049 Camino Dos Rios
P.O. Box 1085
Thousand Oaks, CA 91360

Professor A. E. Miller
University of Notre Dame
College of Engineering
Notre Dame, IN 46556

Dr. Jeff Perkins
Naval Postgraduate School
Monterey, CA 93940

Professor H. W. Pickering
Pennsylvania State University
Department of Material Sciences
University Park, PA 16802

SUPPLEMENTARY DISTRIBUTION LIST
(Continued)

Dr. William R. Prindle
National Academy of Sciences
National Research Council
2101 Constitution Avenue
Washington, DC 20418

Professor R. W. Staehle
Ohio State University
Department of Metallurgical Engineering
Columbus, OH 43210

Dr. Barry C. Syrett
Stanford Research Institute
333 Ravenswood Avenue
Menlo Park, CA 94025

Dr. R. P. Wei
Lehigh University
Institute for Fracture and
Solid Mechanics
Bethlehem, PA 18015

Professor H. G. F. Wilsdorf
University of Virginia
Department of Materials Science
Charlottesville, VA 22903

UNIVERSITY OF VIRGINIA

School of Engineering and Applied Science

The University of Virginia's School of Engineering and Applied Science has an undergraduate enrollment of approximately 1,000 students with a graduate enrollment of 350. There are approximately 120 faculty members, a majority of whom conduct research in addition to teaching.

Research is an integral part of the educational program and interests parallel academic specialties. These range from the classical engineering departments of Chemical, Civil, Electrical, and Mechanical to departments of Biomedical Engineering, Engineering Science and Systems, Materials Science, Nuclear Engineering, and Applied Mathematics and Computer Science. In addition to these departments, there are interdepartmental groups in the areas of Automatic Controls and Applied Mechanics. All departments offer the doctorate; the Biomedical and Materials Science Departments grant only graduate degrees.

The School of Engineering and Applied Science is an integral part of the University (approximately 1,400 full-time faculty with a total enrollment of about 14,000 full-time students), which also has professional schools of Architecture, Law, Medicine, Commerce, and Business Administration. In addition, the College of Arts and Sciences houses departments of Mathematics, Physics, Chemistry and others relevant to the engineering research program. This University community provides opportunities for interdisciplinary work in pursuit of the basic goals of education, research, and public service.